

Adaptive Policy Backbone via Shared Network

Bumgeun Park, Donghwan Lee ^{*}
 Korea Advanced Institute of Science and Technology (KAIST)
 {j4t123, donghwan}@kaist.ac.kr

September 29, 2025

Abstract

Reinforcement learning (RL) has achieved impressive results across domains, yet learning an optimal policy typically requires extensive interaction data, limiting practical deployment. A common remedy is to leverage priors—such as pre-collected datasets or reference policies—but their utility degrades under task mismatch between training and deployment. While prior work has sought to address this mismatch, it has largely been restricted to in-distribution settings. To address this challenge, we propose **Adaptive Policy Backbone** (APB), a meta-transfer RL method that inserts lightweight linear layers before and after a shared backbone, thereby enabling parameter-efficient fine-tuning (PEFT) while preserving prior knowledge during adaptation. Our results show that APB improves sample efficiency over standard RL and adapts to out-of-distribution (OOD) tasks where existing meta-RL baselines typically fail.

1 Introduction

Reinforcement learning (RL) has demonstrated impressive ability to learn high-performing policies across diverse domains, including gaming (Mnih et al., 2015; Vinyals et al., 2019; Berner et al., 2019), robotics (Levine et al., 2016; Akkaya et al., 2019), traffic control (El-Tantawy et al., 2013), and aligning large language models with human preferences (Stiennon et al., 2020). However, learning a high-performing policy in RL typically requires extensive data collection, thereby discouraging practical deployment.

To alleviate the burden of extensive data collection, recent work has explored leveraging *priors*, either via a pre-collected dataset (Levine et al., 2020) or a reference policy (Xie et al., 2021; Kalashnikov et al., 2018). In practice, however, the deployment task often differs from that represented by the dataset or reference policy; such *task mismatch* can substantially diminish the utility of these priors. To leverage priors despite this mismatch, several approaches have been proposed in the context of meta-RL (Wang et al., 2016; Duan et al., 2016; Finn et al., 2017; Rakelly et al., 2019), which aim to leverage prior knowledge for efficient adaptation, either by (i) improving the sample efficiency of standard RL or by (ii) enabling rapid adaptation to new tasks.

Despite progress on handling task mismatch, many methods still struggle with adapting to out-of-distribution (OOD) tasks and thus fail to leverage prior knowledge, because they implicitly

^{*}Corresponding author

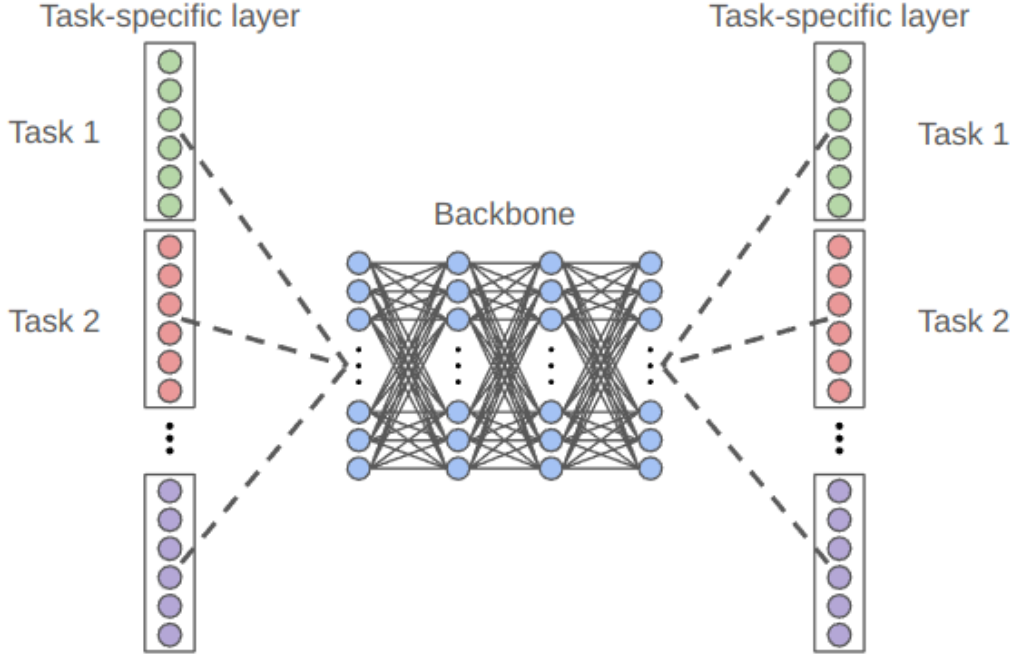


Figure 1: APB architecture: a shared backbone with task-specific linear layers.

assume that training and deployment tasks are drawn from the same distribution, which is rarely realistic. For example, Finn et al. (2017) evaluates policy adaptation on HalfCheetah-v1, where training tasks are reaching target velocities uniformly sampled from $[0, 3]$ and, after training, the policy is adapted to new targets drawn from the same range. However, one typically desires methods that adapt effectively even when tasked with moving backward (negative target velocity), which is fundamentally OOD. This gap highlights the need for methods that reliably adapt to tasks beyond those encountered during training.

In this paper, we propose the **Adaptive Policy Backbone** (APB), a meta-transfer RL method for sample-efficient adaptation on OOD tasks. To address the challenges posed by OOD tasks, we adopt an initialization-based meta-RL paradigm that learns a meta-initialization and adapts via fine-tuning at test time (Beck et al., 2023). As illustrated in Figure 1, APB consists of a backbone shared across meta-training tasks, together with task-specific linear layers placed before and after it. After meta-training the backbone, APB employs parameter-efficient fine-tuning (PEFT), enabling adaptation by updating only the task-specific linear layers while preserving previously acquired knowledge in the backbone. Prior work has investigated PEFT for meta-RL and has reported advantages over full fine-tuning, but primarily within in-distribution settings (Zintgraf et al., 2019; Raghu et al., 2019). In contrast, we focus on OOD task adaptation and provide a theoretical analysis.

Our main claims are as follows. First, training only the pre- and post-backbone linear layers while maintaining the backbone parameters is sufficient to adapt to the new task. To support

our claim, we present a theoretical analysis under a simple setting and provide empirical results on more complex environments. The results show that APB can improve the sample efficiency over the standard RL algorithms and adapts to OOD tasks where existing meta-RL methods typically fail. Second, APB is capable of generalizing behavior on OOD tasks. To validate the generalization capability of APB, we conduct a behavior cloning (BC) evaluation with OOD expert demonstrations whose trajectory distribution is narrowly concentrated, a regime in which vanilla BC typically fails to generalize behavior. From the perspective of leveraging backbone parameters trained on meta-training tasks for enhanced sample efficiency, APB can be interpreted as transfer learning, while it may also be regarded as meta-learning in terms of improving generalization to OOD tasks.

2 Related Works

Parameter-Efficient Fine-Tuning. Fine-tuning is a widely used approach to adapt pre-trained models to downstream tasks by adjusting model parameters. However, full fine-tuning can be inefficient and often leads to catastrophic forgetting, where previously learned knowledge is overwritten and performance deteriorates. Recently, parameter-efficient fine-tuning (PEFT) has emerged as a promising alternative. PEFT enables adaptation to downstream tasks while mitigating catastrophic forgetting, updating only a small subset of parameters and freezing the rest. Previously, PEFT has been implemented by making only adapter parameters learnable (Zhang et al., 2023; Hu et al., 2022; Sung et al., 2022; Houlsby et al., 2019), or by updating only the bias terms (Zaken et al., 2021), a single layer (Lee et al., 2022; Zhu et al., 2023; Kumar et al., 2022), or a layer block (Peng et al., 2024). Due to its effectiveness on downstream tasks, PEFT is utilized in various areas such as LLM (Fu et al., 2023; Zhang et al., 2023; Hu et al., 2022; Houlsby et al., 2019; Zaken et al., 2021; Zhu et al., 2023), vision (Lee et al., 2022; Sung et al., 2022; Kumar et al., 2022; Peng et al., 2024; Jia et al., 2022; Jie and Deng, 2023; Wang et al., 2023), robot learning for sim2real (Truong et al., 2021; Sharma et al., 2023), and meta-RL (Zintgraf et al., 2019; Raghu et al., 2019).

Transfer Learning. Transfer learning (TL) is an approach for transferring knowledge learned in a source domain to accelerate learning in a target domain. Because TL aims to transfer informative representations that improve generalization, these ideas have been applied to meta-RL (Devin et al., 2017; Borsa et al., 2018; Zintgraf et al., 2019; Raghu et al., 2019). Devin et al. (2017) pre-train modular policy components across tasks and dynamically reassemble them for new tasks. Zintgraf et al. (2019); Raghu et al. (2019) pre-train policies and adapt by fine-tuning only a subset of parameters to enable fast adaptation. Borsa et al. (2018) leverage successor features to promote generalization across tasks. However, successor-feature methods can degrade under drastic changes in the reward function across domains, and they typically assume shared transition dynamics (Lehnert et al., 2017; Borsa et al., 2018).

Meta Learning. Meta-learning is a subfield of machine learning that aims to train models across a variety of tasks such that they can rapidly solve new, unseen tasks. The objectives of meta-learning include learning effective parameter initializations (Finn et al., 2017; Ravi and Larochelle, 2017; Nichol et al., 2018), discovering task-specific update rules or learning algorithms (Santoro et al., 2016; Munkhdalai and Yu, 2017; Mishra et al., 2017), and learning task similarity metrics (Koch et al., 2015; Vinyals et al., 2016; Snell et al., 2017; Sung et al., 2018).

Meta-learning has recently been actively investigated in the context of RL, known as meta-RL. Wang et al. (2016); Duan et al. (2016) propose recurrent approaches that encode experience to infer task-specific dynamics. Finn et al. (2017) introduces Model-Agnostic Meta-Learning (MAML), which aims to learn an initial set of parameters that can be quickly adapted to other tasks with a few gradient steps. Several variants of MAML have subsequently been proposed (Nichol et al., 2018; Stadie et al., 2018; Zintgraf et al., 2019; Raghu et al., 2019; Song et al., 2019). Meanwhile, Rakelly et al. (2019); Zintgraf et al. (2019); Beukman et al. (2023); Liang et al. (2024) employ a context encoder to infer task identity from transition history, enabling efficient posterior inference for adaptation. Recently, to improve generalization over task distributions, Xu et al. (2022); Schmied et al. (2023); Wang et al. (2024) utilize the transformer-based architecture (Vaswani et al., 2017).

3 Preliminaries

3.1 Problem Formulation

We consider a Markov decision process (MDP) defined by the tuple $(\mathcal{S}, \mathcal{A}, P, r, \gamma)$. \mathcal{S} is the state space, \mathcal{A} is the action space, $P(\cdot|s, a)$ is the transition kernel over \mathcal{S} , $r : \mathcal{S} \times \mathcal{A} \rightarrow [r_{\min}, r_{\max}]$ is the reward function, and $\gamma \in (0, 1)$ is a discount factor that controls the weighting of future rewards. At each time step t , given state $s_t \in \mathcal{S}$, the agent chooses an action $a_t \in \mathcal{A}$ according to a (possibly stochastic) policy $\pi(a|s)$. The state then transitions from s_t to s_{t+1} according to $P(s_{t+1}|s_t, a_t)$, and the agent receives a reward $r(s_t, a_t)$. Moreover, the state-value function under policy π is defined as

$$v^\pi(s_t) = \mathbb{E}_{\substack{a_k \sim \pi(\cdot|s_k) \\ s_{k+1} \sim P(\cdot|s_k, a_k)}} \left[\sum_{k=t}^{\infty} \gamma^{k-t} r(s_k, a_k) \mid s_t \right]$$

The objective of RL is to learn a policy π that maximizes the expected return $\mathbb{E}_{s_0 \sim \rho_0} [v^\pi(s_0)]$, where ρ_0 denotes the initial-state distribution.

Here, we formalize the meta-RL setting as follows. Let $p(\mathcal{T})$ denote a distribution over tasks, where each task $\mathcal{T}_i \sim p(\mathcal{T})$ corresponds to an MDP $(\mathcal{S}, \mathcal{A}, P, r_{\mathcal{T}}, \gamma)$. In this work, task variation arises from differences in reward functions. During meta-training, we sample N number of tasks $\{\mathcal{T}_i\}_{i=1}^N \sim p(\mathcal{T})$, and interact with these tasks to learn shared parameters. At evaluation, a novel task $\mathcal{T}_o \sim q(\mathcal{T})$ is drawn from a distribution $q(\mathcal{T})$ that differs from $p(\mathcal{T})$ (i.e., OOD with respect to $p(\mathcal{T})$; e.g., $\text{supp}(q) \not\subseteq \text{supp}(p)$).

3.2 Matrix Expression

Although the MDP considered in this paper has continuous spaces, we adopt a discrete setting for matrix-based analysis and slightly overload notation to denote matrix representation. Under policy π , define V^π , R^π and P^π as the state-value vector, the expected reward vector, and the state transition matrix, respectively, presented as follows:

$$V^\pi = \begin{bmatrix} v^\pi(s_1) \\ \vdots \\ v^\pi(s_{|\mathcal{S}|}) \end{bmatrix} \in \mathbb{R}^{|\mathcal{S}| \times 1}, R^\pi = \begin{bmatrix} \mathbb{E}_{a \sim \pi(\cdot|s_1)} [r(s_1, a)] \\ \vdots \\ \mathbb{E}_{a \sim \pi(\cdot|s_{|\mathcal{S}|})} [r(s_{|\mathcal{S}|}, a)] \end{bmatrix} \in \mathbb{R}^{|\mathcal{S}| \times 1}$$

$$P^\pi = \begin{bmatrix} \mathbb{E}_{a \sim \pi(\cdot|s_1)} [P(s_1|s_1, a)] & \cdots & \mathbb{E}_{a \sim \pi(\cdot|s_1)} [P(s_{|\mathcal{S}|}|s_1, a)] \\ \vdots & \ddots & \vdots \\ \mathbb{E}_{a \sim \pi(\cdot|s_{|\mathcal{S}|})} [P(s_1|s_{|\mathcal{S}|}, a)] & \cdots & \mathbb{E}_{a \sim \pi(\cdot|s_{|\mathcal{S}|})} [P(s_{|\mathcal{S}|}|s_{|\mathcal{S}|}, a)] \end{bmatrix} \in \mathbb{R}^{|\mathcal{S}| \times |\mathcal{S}|}$$

Assuming sufficiently long or infinite-horizon episodes, V^π can be expressed as:

$$V^\pi = (I_{|\mathcal{S}|} - \gamma P^\pi)^{-1} R^\pi$$

where $I_{|\mathcal{S}|} \in \mathbb{R}^{|\mathcal{S}| \times |\mathcal{S}|}$ is the identity matrix. Following Wang et al. (2007); Luan et al. (2019); Lim and Lee (2024), let $\Pi \in \mathbb{R}^{|\mathcal{S}| \times |\mathcal{S}||\mathcal{A}|}$ be the policy matrix with $(\Pi)_{s, (s', a)} = \pi(a | s) \mathbf{1}\{s' = s\}$ and the $\mathbf{r} \in \mathbb{R}^{|\mathcal{S}||\mathcal{A}| \times 1}$ the state-action reward vector with $\mathbf{r}_{(s, a)} = r(s, a)$. Then

$$P^\pi = \Pi P, \quad R^\pi = \Pi \mathbf{r}$$

4 Adaptive Policy Backbone

We propose Adaptive Policy Backbone (APB), a simple yet effective meta-transfer RL method designed to improve sample efficiency over standard RL and to enable adaptation to OOD tasks where existing meta-RL methods often fail. We argue that updating only the first and last layers of the policy network—while freezing the backbone to preserve prior knowledge—suffices for effective adaptation to new tasks. The key intuition is that although each optimal policy is task-specific, policies share a common component induced by structural similarities in the underlying MDPs; this shared structure reduces the need for extensive retraining on new tasks. Furthermore, it is well-established that fine-tuning only a subset of parameters can significantly improve sample efficiency and reduce training costs. Structurally, APB is analogous to D’Eramo et al. (2024), which uses a backbone shared across training tasks together with task-specific nonlinear modules placed before and after the backbone. While that line of work emphasizes how shared knowledge aids per-task training, APB replaces the non-linear modules with linear layers for greater parameter efficiency and targets test-time adaptation to OOD tasks in a meta-learning setting. To support our main claim, we provide a theoretical analysis of the policy structure in a simple environment, and extend our study to more complex environments through empirical experiments.

4.1 Theoretical study of the policy structure

We begin our analysis with a simple environment with finite state and action spaces.

Lemma 1. *If $V^\pi = (I_{|\mathcal{S}|} - \gamma P^\pi)^{-1} R^\pi$ holds, then using $P^\pi = \Pi P$ and $R^\pi = \Pi \mathbf{r}$ we have $V^\pi = \Pi(\gamma P V^\pi + \mathbf{r})$. Consequently, the policy matrix Π can be expressed as*

$$\Pi = \frac{V^\pi(\gamma P V^\pi + \mathbf{r})^\top}{\|\gamma P V^\pi + \mathbf{r}\|^2} + N \quad \text{with} \quad N(\gamma P V^\pi + \mathbf{r}) = \mathbf{0}_{|\mathcal{S}|} \quad (1)$$

where $N \in \mathbb{R}^{|\mathcal{S}| \times |\mathcal{S}||\mathcal{A}|}$ has rows orthogonal to $\gamma P V^\pi + \mathbf{r}$.

Lemma 2. *Let Π_1 and Π_2 be the (optimal) policy matrices for task 1 and task 2, respectively, and let $A \in \mathbb{R}^{|\mathcal{S}| \times |\mathcal{S}|}$ satisfy $AV_1 = V_2$. Then there exists $B \in \mathbb{R}^{|\mathcal{S}||\mathcal{A}| \times |\mathcal{S}||\mathcal{A}|}$ such that*

$$A\Pi_1 B = \Pi_2 \quad (2)$$

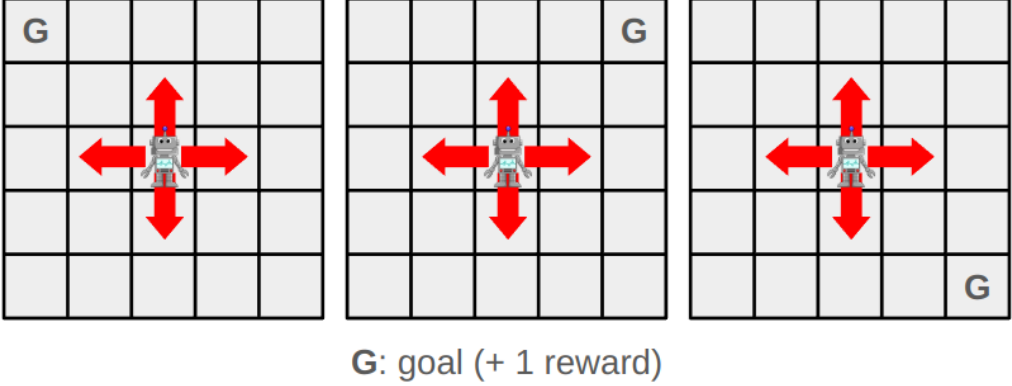


Figure 2: Toy example demonstrating MDPs that are isomorphic under state permutation.

Given Π_1 , we can thus obtain Π_2 by solving for appropriate matrices A and B . To relate Lemma 2 to our main claim, we adopt the following restrictive assumption.

Assumption 1. *A is a permutation matrix (i.e., the two MDPs are isomorphic up to a permutation of the state space).*

An illustrative toy example is provided in Figure 2.

Theorem 1. *Under Assumption 1, if each state s is represented as a one-hot row vector, then the (optimal) policy for task 2 can be written as*

$$\pi_2(\cdot | s) = h(\pi_1(\cdot | g(s))) \quad (3)$$

where $g : \mathbb{R}^{|S|} \rightarrow \mathbb{R}^{|S|}$ is linear (e.g., $g(s) = sA$) and $h : \mathbb{R}^{|A|} \rightarrow \mathbb{R}^{|A|}$ is a (possibly state-dependent) linear map.

Although such isomorphic MDPs are rare in practice, we later show empirically that our method remains effective even beyond this restrictive case.

We parameterize the policy as a composition of linear and nonlinear maps:

$$\pi = f_{\text{linear}}^{\text{out}} \circ f \circ f_{\text{linear}}^{\text{in}} \quad (4)$$

where f denotes a nonlinear backbone, and $f_{\text{linear}}^{\text{in}}/f_{\text{linear}}^{\text{out}}$ are input/output linear transforms. Because linear maps compose associatively, adding linear maps before and after π is equivalent to adding linear maps immediately before and after the backbone. We henceforth *absorb* $f_{\text{linear}}^{\text{out}}$ into h and $f_{\text{linear}}^{\text{in}}$ into g , and write

$$h \circ \pi \circ g = (h \circ f_{\text{linear}}^{\text{out}}) \circ f \circ (f_{\text{linear}}^{\text{in}} \circ g) =: h \circ f \circ g \quad (5)$$

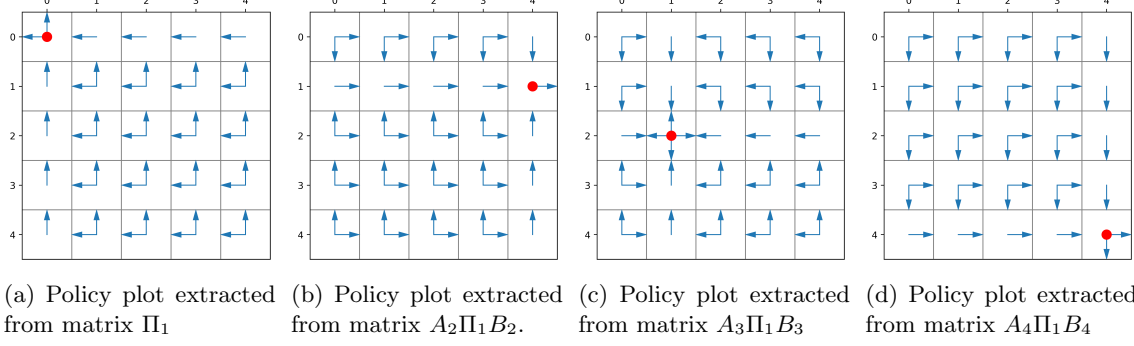


Figure 3: Policy plots for different goal positions depicted by a red dot. An agent choose one of the four actions(up, down, left, right) and when face the wall, it stay. A_i and B_i represent matrix introduced in (16)

4.2 Analysis of Meta-Training Task Coverage and Adaptation Error

We extend our analysis to evaluate adaptation performance on OOD tasks. Let Γ_{train} denote the set of linear transforms (pre-backbone maps) associated with the meta-training tasks. We write

$$\bar{\mathcal{G}} := \{g(s) : g \in \Gamma_{\text{train}}, s \in \mathcal{S}_{\text{meta}}\}$$

for the set of all transformed states observed during meta-training, where $\mathcal{S}_{\text{meta}}$ is the set of states visited under the meta-training policies $\{\pi_t\}_{t=1}^N$ (e.g., the union of the supports of their state-visitation distributions). According to Theorem 1, for any policy backbone f , learning task-specific linear layers g_t (pre-backbone) and h_t (post-backbone) yields a policy for a new task t :

$$\pi_t(\cdot | s) = h_t(f(g_t(s))). \quad (6)$$

However, meta-training yields an approximate backbone f_{meta} that is fitted only to a set of transformed states $g(s) \in \bar{\mathcal{G}}$ and is, in general, not reliable over the entire feature space \mathcal{G} . In particular,

$$f^*(g(s)) \approx f_{\text{meta}}(g(s)) \quad \forall g(s) \in \bar{\mathcal{G}}, \quad (7)$$

where f^* denotes the ideal backbone that is reliable over \mathcal{G} . We assume that, as the diversity of training tasks increases, $\bar{\mathcal{G}} \rightarrow \mathcal{G}$. For a test task t , let $\mathcal{X}_t := \{g_t(s) : s \in \mathcal{S}\}$ be the set of transformed inputs encountered at adaptation time, and let $\mathcal{X}_t^{\text{OOD}} := \mathcal{X}_t \setminus \bar{\mathcal{G}}$. We define the adaptation error as

$$\sum_{x \in \mathcal{X}_t} \|h_t(f^*(x)) - h_t(f_{\text{meta}}(x))\|, \quad x = g_t(s), \quad (8)$$

where $\|\cdot\|$ denotes a vector norm (e.g., the ℓ_2 norm).

Theorem 2. *Suppose both backbone networks f_{meta} and f^* are L -Lipschitz. Then, the adaptation error is bounded as follows:*

$$\sum_{x \in \mathcal{X}_t} \|h_t(f^*(x)) - h_t(f_{\text{meta}}(x))\| \leq 2L\|h_t\|_{\text{op}} \cdot |\mathcal{X}_t^{\text{OOD}}| \cdot \epsilon_{\text{max}} \quad (9)$$

where

- $\|h_t\|_{\text{op}}$ is the operator norm (e.g., spectral norm) of the linear map h_t ,
- $\mathcal{X}_t^{\text{OOD}} = \{x \in \mathcal{X}_t : x \notin \bar{\mathcal{G}}\}$ is the set of test-time inputs not encountered during meta-training,
- $\epsilon_{\max} = \max_{x \in \mathcal{X}_t^{\text{OOD}}} \min_{z \in \bar{\mathcal{G}}} \|x - z\|$ denotes the maximum distance from an OOD input to the meta-training support.

This bound implies that the adaptation error is controlled by both the number of OOD inputs and their distance from the meta-training support, scaled by the Lipschitz constant of the backbone and the operator norm of the head. As the diversity of meta-training tasks increases, the coverage of $\bar{\mathcal{G}}$ grows, thus reducing both $|\mathcal{X}_t^{\text{OOD}}|$ and the typical values of ϵ_{\max} , which in turn tightens the adaptation error bound for novel tasks.

Remark. *Interestingly, we observe that a randomly initialized backbone often induces near-optimal policies on meaningful tasks via suitable linear pre-/post-mappings. A plausible explanation is that a randomly initialized policy may already be (near-)optimal for certain degenerate behavioral tasks; consequently, by Theorem 1, such random initializations can be treated as backbone priors for other tasks. Detailed results are demonstrated in Section A.5.*

5 Experiments

5.1 Experimental Setup

We conduct experiments in the MuJoCo control suite (Todorov et al., 2012) with specific tasks such as reaching goals, or achieving target velocities or directions, which are widely used meta-RL benchmark tasks adopted in previous studies (Finn et al., 2017; Zintgraf et al., 2019; Raghu et al., 2019; Song et al., 2019; Rakelly et al., 2019; Zintgraf et al., 2019; Beukman et al., 2023; Xu et al., 2022; Wang et al., 2024). While our primary focus is task variation induced by reward functions, we also evaluate the algorithm under variations in transition dynamics. In contrast to most prior approaches that assess adaptation primarily on in-distribution tasks, our method is designed to enhance adaptability to OOD tasks, thereby broadening the practical applicability of meta-learning. We mainly adopt the code used in Rakelly et al. (2019) with some modifications to implement OOD test protocols. Detailed task specifications are provided in Section A.2.

We meta-train a shared backbone across meta-training tasks until convergence and, during OOD adaptation, freeze it while adapting task-specific linear layers, using a standard TD3 policy module (Fujimoto et al., 2018). We provide a pseudocode for APB in Algorithm 1, in which M and η denote the number of trajectories to obtain samples and the learning rate. All hyperparameters used in the experiments are listed in Section A.3.

For the experiments comparing with meta-RL baselines, we evaluate our method against two well-established paradigms: (i) parameterized policy-gradient (PPG) methods that adapt via gradient-based fine-tuning of the parameters (MAML, ANIL, CAVIA; (Finn et al., 2017; Raghu et al., 2019; Zintgraf et al., 2019)) and (ii) black-box methods that adapt by *online inference*—they *continually update* a task-latent from the incoming context while keeping network weights fixed at test time (PEARL, VariBAD; (Rakelly et al., 2019; Zintgraf et al., 2019)). We also include the recent transformer-based Meta-DT (Wang et al., 2024).

The experiments are designed to answer the following questions.

Algorithm 1 Adaptive Policy Backbone (APB)

▷ **Meta-training**

Sample n meta-training tasks $\{\mathcal{T}_1, \dots, \mathcal{T}_n\} \sim p(\mathcal{T})$
 Initialize policy: shared backbone parameters ψ , head parameters $\{\rho_i^h\}_{i=1}^n$, tail parameters $\{\rho_i^t\}_{i=1}^n$
 Initialize Q-functions $\{\omega_i\}_{i=1}^n$
while not converged **do**
for $i = 1$ to n **do**
 Roll out episode in \mathcal{T}_i , store transitions in \mathcal{B}_i
 Compute critic loss $\mathcal{L}_i^{\text{critic}}$ and actor loss $\mathcal{L}_i^{\text{actor}}$
 Update critic: $\omega_i \leftarrow \omega_i - \eta \nabla_{\omega_i} \mathcal{L}_i^{\text{critic}}$
 Update actor head/tail: $(\rho_i^h, \rho_i^t) \leftarrow (\rho_i^h, \rho_i^t) - \eta \nabla_{(\rho_i^h, \rho_i^t)} \mathcal{L}_i^{\text{actor}}$
end for
 Update backbone: $\psi \leftarrow \psi - \eta \nabla_{\psi} \left(\frac{1}{n} \sum_{i=1}^n \mathcal{L}_i^{\text{actor}} \right)$
end while

▷ **Meta-testing**

Choose OOD task $\mathcal{T}_o \not\sim p(\mathcal{T})$
 Initialize backbone ψ with pretrained parameters from meta-training (frozen)
 Initialize head ρ^h , tail ρ^t , Q-function ω
while not converged **do**
for $i = 1$ to M **do**
 Roll out episode with $\{\rho^h, \psi, \rho^t\}$ in \mathcal{T}_o , store transitions in \mathcal{B}
end for
 Compute critic loss $\mathcal{L}^{\text{critic}}$ and actor loss $\mathcal{L}^{\text{actor}}$
 Update critic: $\omega \leftarrow \omega - \eta \nabla_{\omega} \mathcal{L}^{\text{critic}}$
 Update actor head/tail: $(\rho^h, \rho^t) \leftarrow (\rho^h, \rho^t) - \eta \nabla_{(\rho^h, \rho^t)} \mathcal{L}^{\text{actor}}$
end while

- Does APB improve sample efficiency over a standard RL algorithm?
- Does APB achieve superior adaptation performance on OOD tasks compared with existing meta-RL baselines?
- Does meta-trained policy backbone generalize to OOD tasks?

5.2 Experimental Results

Improvement of sample efficiency over a standard RL algorithm. One particular property of the meta-RL algorithm is to learn new tasks better than standard RL algorithms (Beck et al., 2023). For this purpose, meta-RL learns priors from many tasks and leverages them to promote the learning process. In our experiment, we compare APB against a strong standard RL baseline TD3 under the same network capacity for fair comparison. Across most tasks, the proposed

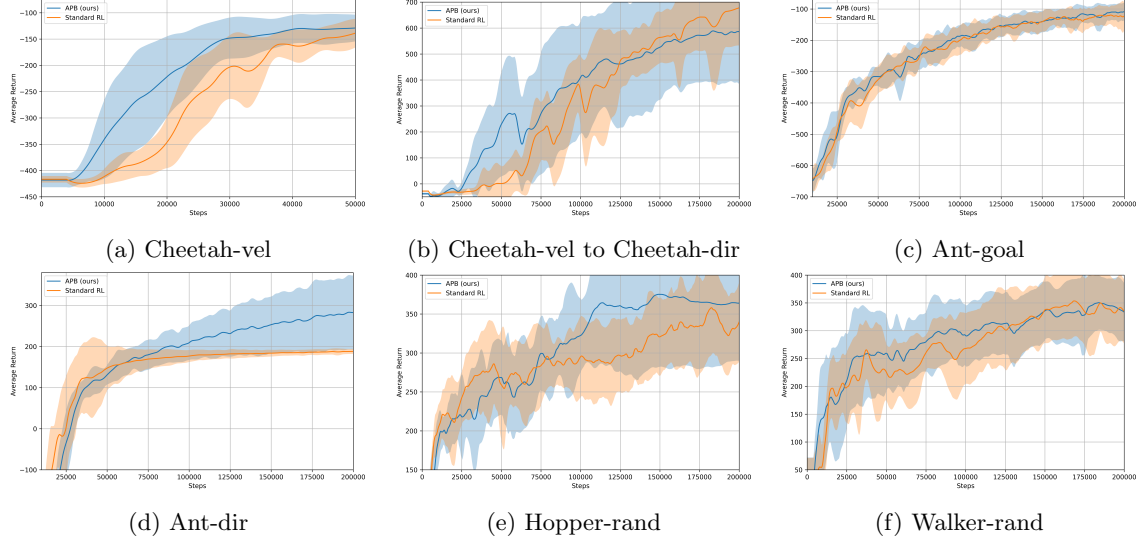


Figure 4: Experimental result comparing APB and the standard RL algorithm on the out-of-distribution tasks. Each curve represents the average return over 10 random seeds, with the shaded area indicating one standard deviation from the mean.

method achieves (marginally) better performance than a standard RL algorithm, exhibiting faster convergence and/or higher asymptotic average return for the same number of interactions. The results are demonstrated in Figure 4 and detailed implementations are presented in Section A.6.

Superior adaptation performance compared with well-established Meta-RL methods. Despite fine-tuning parameters during adaptation, MAML and CAVIA show a negligible increase in average return. ANIL also fine-tunes policy parameters but freezes the backbone during adaptation, similarly to our proposed method. Black-box algorithms such as PEARL, VariBAD, and Meta-DT fail to adapt under reward variation, whereas they show only slight yet consistent gains under transition variation. We hypothesize that this gap arises because transition variation induces only a mild shift in the observation distribution (task semantics and rewards remain largely unchanged), whereas reward variation changes the objective and drives policies into different regions of the state space, yielding OOD observations that the context encoder was not trained to encode. Across all tasks, our method shows consistent adaptation performance. The results are depicted in Figure 5.

Behavior cloning. To assess whether a pretrained policy structure genuinely generalizes to OOD tasks, we perform behavior cloning (BC) (Pomerleau, 1988) on (near-)expert demonstrations collected from OOD tasks. Prior work reports that imitation using expert data often fails to generalize behavior because expert demonstrations cover only a narrow portion of the state-action space (Ross and Bagnell, 2010); accordingly, we deliberately use demonstrations with limited coverage. We train two policies via supervised learning on the same demonstrations: (i) a model that freezes the meta-trained backbone and updates only the task-specific linear layers, and (ii) a randomly initialized model with all parameters unfrozen and updated during training. At evaluation, we roll

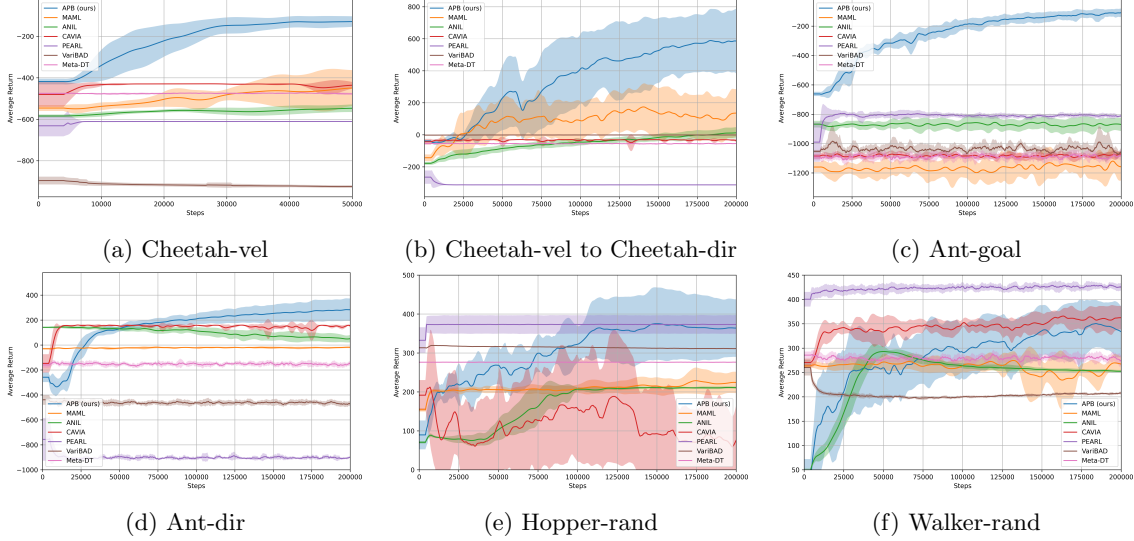


Figure 5: Experimental result comparing APB and the existing meta-RL baselines on the out-of-distribution tasks. Each curve represents the average return over 10 random seeds, with the shaded area indicating one standard deviation from the mean.

out each policy on episodes whose horizon exceeds that of the demonstrations ($H_{\text{eval}} > H_{\text{demo}}$), forcing extrapolation beyond the support of the demonstrations and thereby stressing OOD generalization. As shown in Figure 6, the pretrained backbone improves generalization over the baseline on most tasks. Details of the experimental setup are provided in Section A.4.

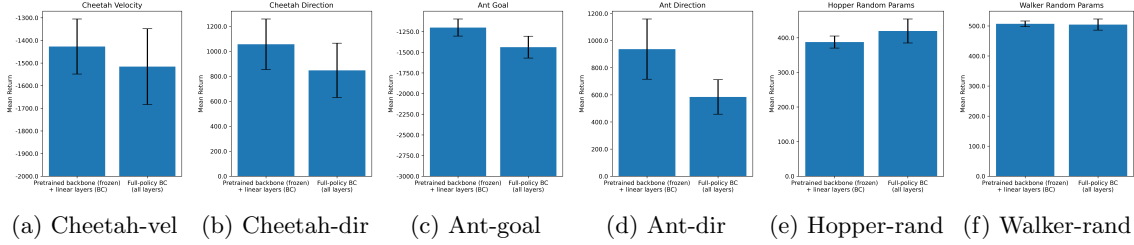


Figure 6: Experimental results on BC. Mean episodic return with 95% confidence intervals across 10 random seeds.

6 Discussion

In this paper, we propose APB, a meta-transfer RL method for OOD task adaptation. Our main claims are twofold: (i) updating only linear layers placed before and after a shared backbone—while keeping the backbone fixed—suffices to adapt to new tasks, and (ii) APB is capable of generalizing

behavior on OOD tasks. We support these claims with a simple theoretical analysis and empirical results on widely used meta-RL benchmarks.

Limitations. APB exhibits potential but also has several limitations. First, this study is limited to state-based observations; extending APB to pixel-based observations (e.g., images) remains important future work. Second, although APB requires fewer trainable parameters than standard RL, it does not yield a significant improvement in sample efficiency; further investigation into adaptation/optimization schemes to accelerate learning is a worthwhile direction. Third, the current policy parameterization (fixed backbone with linear pre-/post-layers) may be limited in expressiveness as the number and diversity of tasks grow, implying a capacity–coverage trade-off. We expect that more expressive architectures such as diffusion models (Ho et al., 2020) or transformers (Vaswani et al., 2017) could address these limitations in future work.

References

Tao Wang, Michael Bowling, and Dale Schuurmans. Dual representations for dynamic programming and reinforcement learning. In *2007 IEEE International Symposium on Approximate Dynamic Programming and Reinforcement Learning*, pages 44–51. IEEE, 2007.

Sitao Luan, Xiao-Wen Chang, and Doina Precup. Revisit policy optimization in matrix form. *arXiv preprint arXiv:1909.09186*, 2019.

Coline Devin, Abhishek Gupta, Trevor Darrell, Pieter Abbeel, and Sergey Levine. Learning modular neural network policies for multi-task and multi-robot transfer. In *2017 IEEE International Conference on Robotics and Automation (ICRA)*, pages 2169–2176. IEEE, 2017.

Adam Santoro, Sergey Bartunov, Matthew Botvinick, Daan Wierstra, and Timothy Lillicrap. Meta-learning with memory-augmented neural networks. In *International Conference on Machine Learning*, pages 1842–1850. PMLR, 2016.

Tsendsuren Munkhdalai and Hong Yu. Meta networks. In *International Conference on Machine Learning*, pages 2554–2563. PMLR, 2017.

Nikhil Mishra, Mostafa Rohaninejad, Xi Chen, and Pieter Abbeel. A simple neural attentive meta-learner. *arXiv preprint arXiv:1707.03141*, 2017.

Gregory Koch, Richard Zemel, and Ruslan Salakhutdinov. Siamese neural networks for one-shot image recognition. In *ICML Deep Learning Workshop*, volume 2, number 1, pages 1–3. Lille, 2015.

Oriol Vinyals, Charles Blundell, Timothy Lillicrap, Daan Wierstra, et al. Matching networks for one shot learning. In *Advances in Neural Information Processing Systems*, volume 29, 2016.

Jake Snell, Kevin Swersky, and Richard Zemel. Prototypical networks for few-shot learning. In *Advances in Neural Information Processing Systems*, volume 30, 2017.

Flood Sung, Yongxin Yang, Li Zhang, Tao Xiang, Philip H.S. Torr, and Timothy M. Hospedales. Learning to compare: Relation network for few-shot learning. In *Proceedings of the IEEE Conference on Computer Vision and Pattern Recognition*, pages 1199–1208, 2018.

Chelsea Finn, Pieter Abbeel, and Sergey Levine. Model-agnostic meta-learning for fast adaptation of deep networks. In *International Conference on Machine Learning*, pages 1126–1135. PMLR, 2017.

Sachin Ravi and Hugo Larochelle. Optimization as a model for few-shot learning. In *International Conference on Learning Representations*, 2017.

Alex Nichol, Joshua Achiam, and John Schulman. On first-order meta-learning algorithms. *arXiv preprint arXiv:1803.02999*, 2018.

Jane X. Wang, Zeb Kurth-Nelson, Dhruva Tirumala, Hubert Soyer, Joel Z. Leibo, Remi Munos, Charles Blundell, Dharshan Kumaran, and Matt Botvinick. Learning to reinforcement learn. *arXiv preprint arXiv:1611.05763*, 2016.

Yan Duan, John Schulman, Xi Chen, Peter L. Bartlett, Ilya Sutskever, and Pieter Abbeel. RL²: Fast reinforcement learning via slow reinforcement learning. *arXiv preprint arXiv:1611.02779*, 2016.

Kate Rakelly, Aurick Zhou, Chelsea Finn, Sergey Levine, and Deirdre Quillen. Efficient off-policy meta-reinforcement learning via probabilistic context variables. In *International Conference on Machine Learning*, pages 5331–5340. PMLR, 2019.

Volodymyr Mnih, Koray Kavukcuoglu, David Silver, Andrei A. Rusu, Joel Veness, Marc G. Bellemare, Alex Graves, Martin Riedmiller, Andreas K. Fidjeland, Georg Ostrovski, et al. Human-level control through deep reinforcement learning. *Nature*, 518(7540):529–533, 2015.

Oriol Vinyals, Igor Babuschkin, Wojciech M. Czarnecki, Michaël Mathieu, Andrew Dudzik, Junyoung Chung, David H. Choi, Richard Powell, Timo Ewalds, Petko Georgiev, et al. Grandmaster level in StarCraft II using multi-agent reinforcement learning. *Nature*, 575(7782):350–354, 2019.

Christopher Berner, Greg Brockman, Brooke Chan, Vicki Cheung, Przemysław Débiak, Christy Dennison, David Farhi, Quirin Fischer, Shariq Hashme, Chris Hesse, et al. Dota 2 with large scale deep reinforcement learning. *arXiv preprint arXiv:1912.06680*, 2019.

Sergey Levine, Chelsea Finn, Trevor Darrell, and Pieter Abbeel. End-to-end training of deep visuomotor policies. *Journal of Machine Learning Research*, 17(39):1–40, 2016.

Ilge Akkaya, Marcin Andrychowicz, Maciek Chociej, Mateusz Litwin, Bob McGrew, Arthur Petron, Alex Paino, Matthias Plappert, Glenn Powell, Raphael Ribas, et al. Solving rubik’s cube with a robot hand. *arXiv preprint arXiv:1910.07113*, 2019.

Samah El-Tantawy, Baher Abdulhai, and Hossam Abdelgawad. Multiagent reinforcement learning for integrated network of adaptive traffic signal controllers (MARLIN-ATSC): methodology and large-scale application on downtown Toronto. *IEEE Transactions on Intelligent Transportation Systems*, 14(3):1140–1150, 2013.

Nisan Stiennon, Long Ouyang, Jeffrey Wu, Daniel Ziegler, Ryan Lowe, Chelsea Voss, Alec Radford, Dario Amodei, and Paul F. Christiano. Learning to summarize with human feedback. In *Advances in Neural Information Processing Systems*, volume 33, pages 3008–3021, 2020.

Scott Fujimoto, David Meger, and Doina Precup. Off-policy deep reinforcement learning without exploration. In *International Conference on Machine Learning*, pages 2052–2062. PMLR, 2019.

Aviral Kumar, Justin Fu, Matthew Soh, George Tucker, and Sergey Levine. Stabilizing off-policy Q-learning via bootstrapping error reduction. In *Advances in Neural Information Processing Systems*, volume 32, 2019.

Yifan Wu, George Tucker, and Ofir Nachum. Behavior regularized offline reinforcement learning. *arXiv preprint arXiv:1911.11361*, 2019.

Xue Bin Peng, Aviral Kumar, Grace Zhang, and Sergey Levine. Advantage-weighted regression: Simple and scalable off-policy reinforcement learning. *arXiv preprint arXiv:1910.00177*, 2019.

Ilya Kostrikov, Ashvin Nair, and Sergey Levine. Offline reinforcement learning with implicit Q-learning. *arXiv preprint arXiv:2110.06169*, 2021.

Joanne Truong, Sonia Chernova, and Dhruv Batra. Bi-directional domain adaptation for sim2real transfer of embodied navigation agents. *IEEE Robotics and Automation Letters*, 6(2):2634–2641, 2021.

Luisa Zintgraf, Kyriacos Shiarlis, Maximilian Igl, Sebastian Schulze, Yarin Gal, Katja Hofmann, and Shimon Whiteson. Fast context adaptation via meta-learning. In *International Conference on Machine Learning*, pages 7693–7702. PMLR, 2019.

Aniruddh Raghu, Maithra Raghu, Samy Bengio, and Oriol Vinyals. Rapid learning or feature reuse? towards understanding the effectiveness of MAML. *arXiv preprint arXiv:1909.09157*, 2019.

Zihao Fu, Haoran Yang, Anthony Man-Cho So, Wai Lam, Lidong Bing, and Nigel Collier. On the effectiveness of parameter-efficient fine-tuning. In *Proceedings of the AAAI Conference on Artificial Intelligence*, volume 37, number 11, pages 12799–12807, 2023.

Ananya Kumar, Aditi Raghunathan, Robbie Jones, Tengyu Ma, and Percy Liang. Fine-tuning can distort pretrained features and underperform out-of-distribution. *arXiv preprint arXiv:2202.10054*, 2022.

Yoonho Lee, Annie S. Chen, Fahim Tajwar, Ananya Kumar, Huaxiu Yao, Percy Liang, and Chelsea Finn. Surgical fine-tuning improves adaptation to distribution shifts. *arXiv preprint arXiv:2210.11466*, 2022.

Renrui Zhang, Jiaming Han, Chris Liu, Peng Gao, Aojun Zhou, Xiangfei Hu, Shilin Yan, Pan Lu, Hongsheng Li, and Yu Qiao. Llama-adapter: Efficient fine-tuning of language models with zero-init attention. *arXiv preprint arXiv:2303.16199*, 2023.

Edward J. Hu, Yelong Shen, Phillip Wallis, Zeyuan Allen-Zhu, Yuanzhi Li, Lu Wang, Shean Wang, Weizhu Chen, et al. LoRA: Low-rank adaptation of large language models. *ICLR*, 1(2):3, 2022.

Yi-Lin Sung, Jaemin Cho, and Mohit Bansal. VL-adapter: Parameter-efficient transfer learning for vision-and-language tasks. In *Proceedings of the IEEE/CVF Conference on Computer Vision and Pattern Recognition*, pages 5227–5237, 2022.

Neil Houlsby, Andrei Giurgiu, Stanislaw Jastrzebski, Bruna Morrone, Quentin De Laroussilhe, Andrea Gesmundo, Mona Attariyan, and Sylvain Gelly. Parameter-efficient transfer learning for NLP. In *International Conference on Machine Learning*, pages 2790–2799. PMLR, 2019.

Elad Ben Zaken, Shauli Ravfogel, and Yoav Goldberg. BitFit: Simple parameter-efficient fine-tuning for transformer-based masked language-models. *arXiv preprint arXiv:2106.10199*, 2021.

Ligeng Zhu, Lanxiang Hu, and Ji Lin. LIFT: Efficient layer-wise fine-tuning for large model models. 2023.

Zelin Peng, Zhengqin Xu, Zhilin Zeng, Lingxi Xie, Qi Tian, and Wei Shen. Parameter efficient fine-tuning via cross block orchestration for Segment Anything Model. In *Proceedings of the IEEE/CVF Conference on Computer Vision and Pattern Recognition*, pages 3743–3752, 2024.

Menglin Jia, Luming Tang, Bor-Chun Chen, Claire Cardie, Serge Belongie, Bharath Hariharan, and Ser-Nam Lim. Visual prompt tuning. In *European Conference on Computer Vision*, pages 709–727. Springer, 2022.

Shibo Jie and Zhi-Hong Deng. FACT: Factor-tuning for lightweight adaptation on vision transformer. In *Proceedings of the AAAI Conference on Artificial Intelligence*, volume 37, number 1, pages 1060–1068, 2023.

Yaoming Wang, Bowen Shi, Xiaopeng Zhang, Jin Li, Wenrui Dai, Yuchen Liu, Chenglin Li, Hongkai Xiong, and Qi Tian. Adapting shortcut with normalizing flow: An efficient tuning framework for visual recognition. In *2023 IEEE/CVF Conference on Computer Vision and Pattern Recognition (CVPR)*, pages 15965–15974. IEEE, 2023.

Mohit Sharma, Claudio Fantacci, Yuxiang Zhou, Skanda Koppula, Nicolas Heess, Jon Scholz, and Yusuf Aytar. Lossless adaptation of pretrained vision models for robotic manipulation. *arXiv preprint arXiv:2304.06600*, 2023.

Diana Borsa, André Barreto, John Quan, Daniel Mankowitz, Rémi Munos, Hado Van Hasselt, David Silver, and Tom Schaul. Universal successor features approximators. *arXiv preprint arXiv:1812.07626*, 2018.

Lucas Lehnert, Stefanie Tellex, and Michael L. Littman. Advantages and limitations of using successor features for transfer in reinforcement learning. *arXiv preprint arXiv:1708.00102*, 2017.

Bradly C. Stadie, Ge Yang, Rein Houthooft, Xi Chen, Yan Duan, Yuhuai Wu, Pieter Abbeel, and Ilya Sutskever. Some considerations on learning to explore via meta-reinforcement learning. *arXiv preprint arXiv:1803.01118*, 2018.

Xingyou Song, Wenbo Gao, Yuxiang Yang, Krzysztof Choromanski, Aldo Pacchiano, and Yunhao Tang. ES-MAML: Simple hessian-free meta learning. *arXiv preprint arXiv:1910.01215*, 2019.

Zhi Wang, Li Zhang, Wenhao Wu, Yuanheng Zhu, Dongbin Zhao, and Chunlin Chen. Meta-DT: Offline meta-RL as conditional sequence modeling with world model disentanglement. In *Advances in Neural Information Processing Systems*, volume 37, pages 44845–44870, 2024.

Mengdi Xu, Yikang Shen, Shun Zhang, Yuchen Lu, Ding Zhao, Joshua Tenenbaum, and Chuang Gan. Prompting decision transformer for few-shot policy generalization. In *International Conference on Machine Learning*, pages 24631–24645. PMLR, 2022.

Thomas Schmied, Markus Hofmarcher, Fabian Paischer, Razvan Pascanu, and Sepp Hochreiter. Learning to modulate pre-trained models in RL. In *Advances in Neural Information Processing Systems*, volume 36, pages 38231–38265, 2023.

Ashish Vaswani, Noam Shazeer, Niki Parmar, Jakob Uszkoreit, Llion Jones, Aidan N. Gomez, Łukasz Kaiser, and Illia Polosukhin. Attention is all you need. In *Advances in Neural Information Processing Systems*, volume 30, 2017.

Luisa Zintgraf, Kyriacos Shiarlis, Maximilian Igl, Sebastian Schulze, Yarin Gal, Katja Hofmann, and Shimon Whiteson. VariBAD: A very good method for Bayes-adaptive deep RL via meta-learning. *arXiv preprint arXiv:1910.08348*, 2019.

Anthony Liang, Guy Tennenholz, Chih-Wei Hsu, Yinlam Chow, Erdem Biyik, and Craig Boutilier. DynaMITE-RL: A dynamic model for improved temporal meta-reinforcement learning. In *Advances in Neural Information Processing Systems*, volume 37, pages 141390–141416, 2024.

Michael Beukman, Devon Jarvis, Richard Klein, Steven James, and Benjamin Rosman. Dynamics generalisation in reinforcement learning via adaptive context-aware policies. In *Advances in Neural Information Processing Systems*, volume 36, pages 40167–40203, 2023.

Jacob Beck, Risto Vuorio, Evan Zheran Liu, Zheng Xiong, Luisa Zintgraf, Chelsea Finn, and Shimon Whiteson. A survey of meta-reinforcement learning. *arXiv preprint arXiv:2301.08028*, 2023.

Flood Sung, Li Zhang, Tao Xiang, Timothy M. Hospedales, and Yongxin Yang. Learning to learn: Meta-critic networks for sample efficient learning. *arXiv preprint arXiv:1706.09529*, 2017.

Han-Dong Lim and Donghwan Lee. Regularized Q-learning. In *Advances in Neural Information Processing Systems*, volume 37, pages 129855–129887, 2024.

Carlo D’Eramo, Davide Tateo, Andrea Bonarini, Marcello Restelli, and Jan Peters. Sharing knowledge in multi-task deep reinforcement learning. *arXiv preprint arXiv:2401.09561*, 2024.

Matthias Plappert, Rein Houthooft, Prafulla Dhariwal, Szymon Sidor, Richard Y. Chen, Xi Chen, Tamim Asfour, Pieter Abbeel, and Marcin Andrychowicz. Parameter space noise for exploration. *arXiv preprint arXiv:1706.01905*, 2017.

Scott Fujimoto, Herke Hoof, and David Meger. Addressing function approximation error in actor-critic methods. In *International Conference on Machine Learning*, pages 1587–1596. PMLR, 2018.

Anirudh Vemula, Wen Sun, and J. Andrew Bagnell. Contrasting exploration in parameter and action space: A zeroth-order optimization perspective. In *The 22nd International Conference on Artificial Intelligence and Statistics*, pages 2926–2935. PMLR, 2019.

Stéphane Ross and Drew Bagnell. Efficient reductions for imitation learning. In *Proceedings of the Thirteenth International Conference on Artificial Intelligence and Statistics*, pages 661–668. JMLR Workshop and Conference Proceedings, 2010.

Dean A. Pomerleau. ALVINN: An autonomous land vehicle in a neural network. In *Advances in Neural Information Processing Systems*, volume 1, 1988.

Jonathan Ho, Ajay Jain, and Pieter Abbeel. Denoising diffusion probabilistic models. In *Advances in Neural Information Processing Systems*, volume 33, pages 6840–6851, 2020.

Sergey Levine, Aviral Kumar, George Tucker, and Justin Fu. Offline reinforcement learning: Tutorial, review, and perspectives on open problems. *arXiv preprint arXiv:2005.01643*, 2020.

Tengyang Xie, Nan Jiang, Huan Wang, Caiming Xiong, and Yu Bai. Policy finetuning: Bridging sample-efficient offline and online reinforcement learning. In *Advances in Neural Information Processing Systems*, volume 34, pages 27395–27407, 2021.

Dmitry Kalashnikov, Alex Irpan, Peter Pastor, Julian Ibarz, Alexander Herzog, Eric Jang, Deirdre Quillen, Ethan Holly, Mrinal Kalakrishnan, Vincent Vanhoucke, et al. Scalable deep reinforcement learning for vision-based robotic manipulation. In *Conference on Robot Learning*, pages 651–673. PMLR, 2018.

Emanuel Todorov, Tom Erez, and Yuval Tassa. MuJoCo: A physics engine for model-based control. In *2012 IEEE/RSJ International Conference on Intelligent Robots and Systems*, pages 5026–5033. IEEE, 2012.

Evgenii Nikishin, Max Schwarzer, Pierluca D’Oro, and Pierre-Luc Bacon. The primacy bias in deep reinforcement learning. In *International Conference on Machine Learning*, pages 16828–16847. PMLR, 2022.

A Appendix

A.1 Proof

A.1.1 Proof of Lemma 1

Lemma 1. *If $V^\pi = (I_{|\mathcal{S}|} - \gamma P^\pi)^{-1} R^\pi$ holds, then using $P^\pi = \Pi P$ and $R^\pi = \Pi \mathbf{r}$ we have $V^\pi = \Pi(\gamma PV^\pi + \mathbf{r})$. Consequently, the policy matrix Π can be expressed as*

$$\Pi = \frac{V^\pi(\gamma PV^\pi + \mathbf{r})^\top}{\|\gamma PV^\pi + \mathbf{r}\|^2} + N \quad \text{with} \quad N(\gamma PV^\pi + \mathbf{r}) = \mathbf{0}_{|\mathcal{S}|} \quad (10)$$

where $N \in \mathbb{R}^{|\mathcal{S}| \times |\mathcal{S}| \times |\mathcal{A}|}$ has rows orthogonal to $\gamma PV^\pi + \mathbf{r}$.

Proof. From the definition,

$$V^\pi = (I_{|\mathcal{S}|} - \gamma P^\pi)^{-1} R^\pi = (I_{|\mathcal{S}|} - \gamma \Pi P)^{-1} \Pi \mathbf{r} \quad (11)$$

$$\rightarrow (I_{|\mathcal{S}|} - \gamma \Pi P) V^\pi = \Pi \mathbf{r} \quad (12)$$

$$V^\pi - \gamma \Pi P V^\pi = \Pi \mathbf{r} \quad (13)$$

$$\Pi(\mathbf{r} + \gamma P V^\pi) = V^\pi \quad (14)$$

Equation (14) represents a linear system, which admits a general solution and a particular solution. Therefore,

$$\Pi = \frac{V^\pi (\gamma P V^\pi + \mathbf{r})^\top}{\|\gamma P V^\pi + \mathbf{r}\|^2} + N, \quad \text{such that} \quad N(\gamma P V^\pi + \mathbf{r}) = \mathbf{0}_{|\mathcal{S}|} \quad (15)$$

□

A.1.2 Proof of Lemma 2

Lemma 2. *Let Π_1 and Π_2 be the (optimal) policy matrices for task 1 and task 2, respectively, and let $A \in \mathbb{R}^{|\mathcal{S}| \times |\mathcal{S}|}$ satisfy $AV_1 = V_2$. Then there exists $B \in \mathbb{R}^{|\mathcal{S}||\mathcal{A}| \times |\mathcal{S}||\mathcal{A}|}$ such that*

$$A\Pi_1 B = \Pi_2 \quad (16)$$

Proof. We start from the decomposition of Π_1 and Π_2 :

$$\Pi_1 = \frac{V_1 (\gamma P V_1 + r_1)^\top}{\|\gamma P V_1 + r_1\|^2} + N_1, \quad (17)$$

$$\Pi_2 = \frac{V_2 (\gamma P V_2 + r_2)^\top}{\|\gamma P V_2 + r_2\|^2} + N_2 \quad (18)$$

Choose A so that $AV_1 = V_2$, and define

$$B = \frac{(\gamma P V_1 + r_1)(\gamma P V_2 + r_2)^\top}{\|\gamma P V_2 + r_2\|^2} \quad (19)$$

Then

$$A\Pi_1 B = A \frac{V_1 (\gamma P V_1 + r_1)^\top}{\|\gamma P V_1 + r_1\|^2} B + A N_1 B \quad (20)$$

$$= \frac{V_2 (\gamma P V_1 + r_1)^\top}{\|\gamma P V_1 + r_1\|^2} B + A N_1 B \quad (21)$$

$$= \frac{V_2 (\gamma P V_2 + r_2)^\top}{\|\gamma P V_2 + r_2\|^2} + A N_1 \underbrace{\frac{(\gamma P V_1 + r_1)(\gamma P V_2 + r_2)^\top}{\|\gamma P V_2 + r_2\|^2}}_{\text{rows orthogonal to } (\gamma P V_2 + r_2)} \quad (22)$$

For the residual term, right-multiplying by $(\gamma P V_2 + r_2)$ yields

$$A N_1 \frac{(\gamma P V_1 + r_1)(\gamma P V_2 + r_2)^\top}{\|\gamma P V_2 + r_2\|^2} (\gamma P V_2 + r_2) = A N_1 (\gamma P V_1 + r_1) \quad (23)$$

$$= A \mathbf{0}_{|\mathcal{S}|} = \mathbf{0}_{|\mathcal{S}|}, \quad (24)$$

so its rows are orthogonal to $(\gamma PV_2 + r_2)$. Hence, setting

$$N_2 := AN_1 \frac{(\gamma PV_1 + r_1)(\gamma PV_2 + r_2)^\top}{\|\gamma PV_2 + r_2\|^2} \quad (25)$$

gives

$$A\Pi_1 B = \frac{V_2 (\gamma PV_2 + r_2)^\top}{\|\gamma PV_2 + r_2\|^2} + N_2 = \Pi_2. \quad (26)$$

□

A.1.3 Proof of Theorem 1

Theorem 1. *Under Assumption 1, if each state s is represented as a one-hot row vector, then the (optimal) policy for task 2 can be written as*

$$\pi_2(\cdot | s) = h\left(\pi_1(\cdot | g(s))\right) \quad (27)$$

where $g : \mathbb{R}^{|\mathcal{S}|} \rightarrow \mathbb{R}^{|\mathcal{S}|}$ is linear (e.g., $g(s) = sA$) and $h : \mathbb{R}^{|\mathcal{A}|} \rightarrow \mathbb{R}^{|\mathcal{A}|}$ is a (possibly state-dependent) linear map.

Proof. Let $\tilde{\pi}(s)$ be the extended form of policy $\tilde{\pi}(s) : \mathbb{R}^{1 \times |\mathcal{S}|} \rightarrow \mathbb{R}^{1 \times |\mathcal{S}||\mathcal{A}|}$, where only the entries corresponding to state s are nonzero, representing the action probabilities. All other entries are zero. For example, if $|\mathcal{S}| = 2, |\mathcal{A}| = 2$, and the input state is s_1 , then the policy network outputs

$$\tilde{\pi}(s_1) = [\pi(a_1 | s_1), \pi(a_2 | s_1), 0, 0]$$

and for s_2 , the output is

$$\tilde{\pi}(s_2) = [0, 0, \pi(a_1 | s_2), \pi(a_2 | s_2)]$$

Let $EXT(\cdot)$ be the policy extraction operator such that $EXT(\tilde{\pi}(s)) = \pi(\cdot | s)$. Since the state is represented as a one-hot vector, we have:

$$s\Pi = \tilde{\pi}(s) \quad (28)$$

Because $\Pi_2 = A\Pi_1 B$, we have

$$\pi_2(\cdot | s_i) = EXT(\tilde{\pi}_2(s_i)) \quad (29)$$

$$= EXT(s_i \Pi_2) \quad (30)$$

$$= EXT(s_i A \Pi_1 B) \quad (31)$$

Write $s_i A = s_k$ (i.e., A maps the row corresponding to s_i to that of s_k). Then

$$\pi_2(\cdot | s_i) = EXT(s_k \Pi_1 B) \quad (32)$$

$$= EXT(\tilde{\pi}_1(s_k) B) \quad (33)$$

Since $\tilde{\pi}_1(s_k)$ has support only on the k -th state block, $\tilde{\pi}_1(s_k) B$ depends solely on the k -th row block of B . Hence, regardless of the specific extraction mechanism, applying EXT returns a $|\mathcal{A}|$ -dimensional *linear* image of $\pi_1(\cdot | s_k)$; that is, there exists a matrix $B' \in \mathbb{R}^{|\mathcal{A}| \times |\mathcal{A}|}$ such that

$$EXT(\tilde{\pi}_1(s_k) B) = \pi_1(\cdot | s_k) B' \quad (34)$$

We define g by $g(s_i) = s_k$ (equivalently, $s_i A = s_k$), and define h by $h(\pi(\cdot | s)) = \pi(\cdot | s) B'$. With these definitions, we can express π_2 as the composition $h \circ \pi_1 \circ g$, which completes the argument. □

A.1.4 Proof of Theorem 2

Theorem 2. Suppose both backbone networks f_{meta} and f^* are L -Lipschitz. Then, the adaptation error is bounded as follows:

$$\sum_{x \in \mathcal{X}_t} \|h_t(f^*(x)) - h_t(f_{meta}(x))\| \leq 2L\|h_t\|_{op} \cdot |\mathcal{X}_t^{OOD}| \cdot \epsilon_{max} \quad (35)$$

Proof.

$$\begin{aligned} & \sum_{g_t(s) \in \mathcal{G}} \left\| h_t(f^*(g_t(s))) - h_t(f_{meta}(g_t(s))) \right\| \\ &= \sum_{g_t(s) \in \mathcal{G}} \left\| h_t(f^*(g_t(s)) - f_{meta}(g_t(s))) \right\| \end{aligned} \quad (36)$$

$$\leq \|h_t\|_{op} \cdot \sum_{g_t(s) \in \mathcal{G}} \left\| f^*(g_t(s)) - f_{meta}(g_t(s)) \right\| \quad (37)$$

$$\begin{aligned} & \leq \|h_t\|_{op} \cdot \sum_{g_t(s) \in \mathcal{G}} \left(\underbrace{\left\| f^*(g_t(s)) - f^*(\hat{g}_t(s) + \epsilon(s)) \right\|}_{\leq L\|\epsilon(s)\|} \right. \\ & \quad \left. + \underbrace{\left\| f^*(\hat{g}_t(s) + \epsilon(s)) - f_{meta}(\hat{g}_t(s) + \epsilon(s)) \right\|}_{=0} \right. \\ & \quad \left. + \underbrace{\left\| f_{meta}(\hat{g}_t(s) + \epsilon(s)) - f_{meta}(g_t(s)) \right\|}_{\leq L\|\epsilon(s)\|} \right) \end{aligned} \quad (38)$$

$$\text{where } \hat{g}_t(s) = \arg \min_{g'(s) \in \bar{\mathcal{G}}} (\|g_t(s) - g'(s)\|), \quad \epsilon(s) = g_t(s) - \hat{g}_t(s)$$

$$\leq 2L\|h_t\|_{op} \cdot \sum_{g_t(s) \in \bar{\mathcal{G}}^0} \|\epsilon(s)\| \quad (39)$$

$$\leq 2L\|h_t\|_{op} \cdot |\bar{\mathcal{G}}^0| \cdot \epsilon_{max} \quad (40)$$

□

A.2 Task description

Table 1: Task description

	Task (objective)	Meta train	Meta test
Reward	Cheetah-vel (Reaching velocity (v))	$v \sim \mathcal{U}(0.0, 3.0)$	$v = -2.0$
	Cheetah-vel to Cheetah-dir (Going target direction)	$v \sim \mathcal{U}(0.0, 3.0)$	backward
	Ant-goal (Reaching goal position (x, y))	$\theta \sim \mathcal{U}(0, \pi)$ $x, y = 3 \cos \theta, 3 \sin \theta$	$\theta = 1.5\pi$ $x, y = 3 \cos \theta, 3 \sin \theta$
	Ant-dir (Going target direction (θ))	$\theta \sim \mathcal{U}(0, \pi)$	$\theta = 1.5\pi$
Dynamics	Hopper-rand (Going forward)	$\alpha \sim \mathcal{U}(-3.0, 2.1)$ $1.5^\alpha \times \text{body mass}$	$\alpha = 2.4$ $1.5^\alpha \times \text{body mass}$
	Walker-rand (Going forward)	$1.5^\alpha \times \text{body inertia}$ $1.3^\alpha \times \text{damping}$	$1.5^\alpha \times \text{body inertia}$ $1.3^\alpha \times \text{damping}$

Cheetah-vel task. The agent is required to reach a target velocity v using a cheetah model. During meta-training, target velocities are uniformly sampled from $\mathcal{U}(0.0, 3.0)$, and in meta-test, the agent is evaluated at $v = -2.0$.

Cheetah-vel to Cheetah-dir task. This task is designed to evaluate the generalization from the Cheetah-vel to the Cheetah-dir setting. The agent is trained to move in randomly sampled target velocities $v \sim \mathcal{U}(0.0, 3.0)$ during meta-training and is tested in the backward direction during meta-test.

Ant-goal task. The ant agent is required to reach a goal position (x, y) located on a semicircle of radius 3. For meta-training, the target angle θ is sampled uniformly from $[0, \pi]$ and the corresponding goal is set as $x = 3 \cos \theta, y = 3 \sin \theta$. In meta-test, the agent is evaluated at $\theta = 1.5\pi$, that is, $x = 3 \cos \theta, y = 3 \sin \theta$.

Ant-dir task. In this task, the ant must move in a specified direction θ . During meta-training, the direction is uniformly sampled from $\mathcal{U}(0, \pi)$. In meta-test, the agent is evaluated at a fixed direction $\theta = 1.5\pi$.

Hopper-rand task. The agent is required to move forward while adapting to variations in the dynamics. During meta-training, the body mass, inertia, and damping parameters are randomized according to the factor $\alpha \sim \mathcal{U}(-3.0, 2.1)$, with each parameter scaled as $1.5^\alpha \times \text{body mass}$, $1.5^\alpha \times \text{body inertia}$, and $1.3^\alpha \times \text{damping}$. In meta-test, the agent is evaluated with $\alpha = 2.4$.

Walker-rand task. Similar to Hopper-rand task, the walker agent must move forward and adapt to dynamic variations. During meta-training, mass, inertia, and damping are scaled with $\alpha \sim \mathcal{U}(-3.0, 2.1)$, and at meta-test, the parameters are set using $\alpha = 2.4$.

Table 2: Hyperparameters for adaptation

Hyperparameter	Value(s)
Number of trajectories	10
Parameter noise	0.00008 (Cheetah-dir); 0.005 (Cheetah-vel); 0.006 (Ant-goal); 0.00075 (Ant-dir); 0.007 (Hopper-rand); 0.03 (Walker-rand)
Policy initialization coefficient	0.07 (Ant-dir); 0.1 (Hopper-rand); 0.01 (Walker-rand); 0.001 (Others)
Reset episode	15 (Cheetah-vel); 25 (Ant-goal); 10 (Others)
Number of updates	1000 (Cheetah-dir, Ant-dir); 2000 (Others)
Batch size	512
Buffer size	200000
Learning rate	0.0001 (Actor); 0.05 (Critic)
Number of meta-train tasks	30

A.3 Hyperparameters

We provide brief explanations of several hyperparameters below:

- **Number of trajectories:** Number of trajectories sampled before running an update block.
- **Parameter noise:** Standard deviation of the parameter-perturbation noise applied during data collection.
- **Policy initialization coefficient:** Scale factor for initializing the task-specific linear layers; smaller coefficient keeps the layers near zero and stabilizes early adaptation.
- **Reset episodes:** To mitigate early overfitting, we reinitialize the task-specific parameters every n episodes (the “reset” technique (Nikishin et al., 2022)).
- **Number of updates:** Number of gradient update steps performed after each data-collection phase (i.e., after sampling n_{traj} trajectories).

A.4 Behavior cloning

Demonstrations. We collect (near-)expert demonstrations $\mathcal{D}_t = \{(s, a)\}_{i=1}^N$ for each *OOD* test task by rolling out a (near-)expert policy π_{exp} . Each per-task dataset contains $N = 100,000$ state-action pairs (transitions) aggregated across multiple episodes. The demonstrations consist of contiguous expert rollouts with episode horizon H_{demo} and therefore concentrate mass on the expert visitation distribution $d^{\pi_{\text{exp}}}$ (narrow state-action support).

Policy parameterizations. We evaluate two models trained on the same demonstrations.

- **APB-BC (ours).** The meta-trained backbone f_{meta} is *frozen*. We learn only the task-specific linear layers g (pre-backbone) and h (post-backbone). Both layers are initialized with scale w from Table 2.

- **Full model (baseline).** Identical architecture but *randomly initialized*; all parameters are unfrozen and updated during training.

Objective. Following standard continuous-control BC, we use a deterministic policy and minimize the mean-squared error between actions and expert actions:

$$\mathcal{L}_{\text{BC}}(\theta) = \frac{1}{|\mathcal{B}|} \sum_{(s,a) \in \mathcal{B}} \|\pi_\theta(s) - a\|_2^2,$$

where \mathcal{B} is a mini-batch. (For completeness, a stochastic alternative is the negative log-likelihood $\mathcal{L}_{\text{NLL}}(\theta) = -\frac{1}{|\mathcal{B}|} \sum \log \pi_\theta(a | s)$, but we do not use it in our experiments.)

Optimization and preprocessing. We optimize with Adam (PyTorch), a mini-batch size of 2048, using *task-dependent* learning rates:

$$\text{LR} = \begin{cases} 5 \times 10^{-4}, & \text{Walker-rand-params} \\ 1 \times 10^{-4}, & \text{Hopper-rand-params} \\ 1 \times 10^{-3}, & \text{All other tasks (Cheetah-dir, Cheetah-vel, Ant-goal, Ant-dir).} \end{cases} \quad (41)$$

Evaluation. After training, we roll out each policy for episodes with horizon $H_{\text{eval}} > H_{\text{demo}}$ to stress extrapolation beyond the demonstration support (OOD generalization). Performance is measured by episodic return. We report the mean across 10 random seeds and 95% confidence intervals.

A.5 Random initialization for backbone

Motivation. As suggested in Theorem 1, linear pre-/post-mappings can transport policies across tasks. Empirically, we find that even a *randomly initialized* backbone can, with suitable linear layers, induce *near-optimal* behavior on some meaningful tasks. Intuitively, a random backbone implements a fixed random feature map; for certain “degenerate” behavioral objectives, a linear head on top of such features can already be (near-)optimal. If so, the random backbone can serve as a *backbone prior* for other tasks via task-specific linear layers.

Protocol. We randomly initialize a backbone, freeze all backbone parameters, and train only the task-specific linear layers g (pre-backbone) and h (post-backbone). We refer to this variant as **APB (random init)**. Unless noted otherwise, we use the same adaptation budgets and per-task hyperparameters as in the main APB experiments (Table 2); layer scales are initialized with the policy initialization coefficient from the table.

Results. Across all evaluated environments, as shown in Figure 7, *APB (random init)* yields competent performance, although it does not attain the optimal policy. Notably, on ANT-GOAL the method approaches near-optimal performance with only a small gap. These findings support our remark that a randomly initialized backbone can function as a useful *backbone prior* when paired with task-specific linear layers.

Practical takeaway. If meta-training is infeasible, *APB (random init)* is a surprisingly strong and cheap baseline: use a sufficiently wide backbone, freeze it, and adapt only linear layers.

Reproducibility details. We use identical optimizers and update schedules as in the APB adaptation runs (per-task learning rates and update counts in Table 2); only the backbone source differs (random vs. meta-trained).

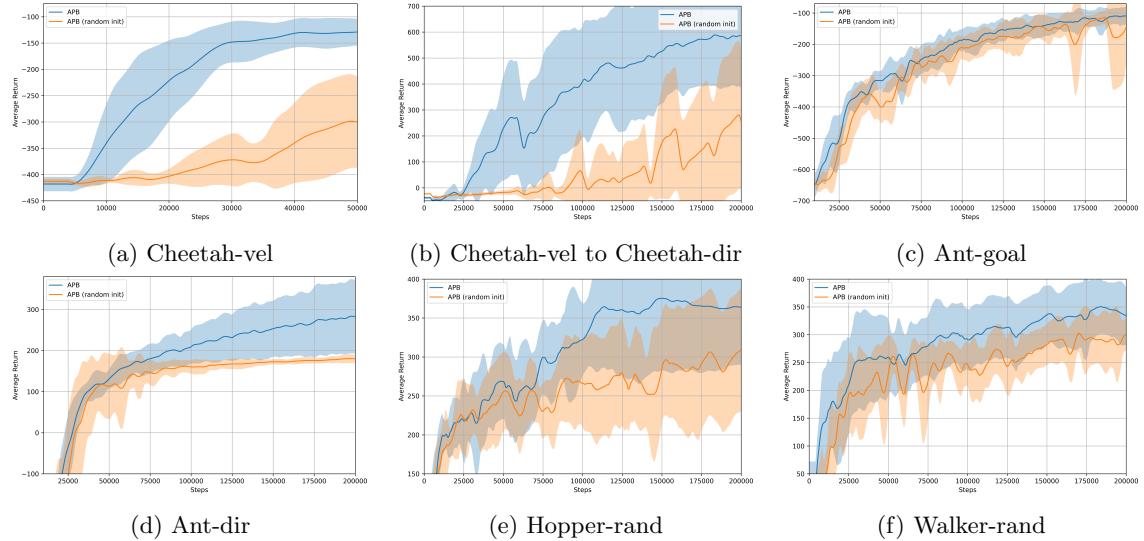


Figure 7: Experimental result comparing APB with pretrained backbone and APB with random initialization on the out-of-distribution tasks. Each curve represents the average return over 10 random seeds, with the shaded area indicating one standard deviation from the mean.

A.6 Practical implementation of APB

During meta-training, a single policy backbone is shared across all tasks, with task-specific *linear layers* placed before and after the backbone; each task also has its own Q-functions (critics). After meta-training, we freeze the backbone and train new task-specific linear layers on the meta-test task using the same optimization pipeline; unlike meta-training, only this small subset of policy parameters is updated at adaptation time. To encourage sufficiently rich exploration with few trainable parameters, we consider two exploration protocols *separately*: (i) evolutionary-style *parameter-space perturbation* (Plappert et al., 2017), and (ii) *action-space* Gaussian noise in the style of TD3 (noise added to the mean action) (Fujimoto et al., 2018). For a fair comparison with standard RL, both APB and the standard RL baseline are evaluated under *both* exploration variants using identical budgets; unless otherwise noted, Figure 4 reports, for each method, the better-performing variant on each task. To mitigate early overfitting of the task-specific adapters, we also adopt a *reset* strategy that periodically reinitializes these parameters every n episodes (Nikishin et al., 2022); the same schedule is used for APB and the standard RL baseline. Unless

otherwise stated, APB and the standard RL baseline share identical training budgets (environment steps, number of updates, batch size, random seeds) and the same evaluation protocol.

A.7 Implementation of meta-RL baselines

We use the authors' public implementations *and* their default hyperparameters for all baselines: MAML (Finn et al., 2017), CAVIA (Zintgraf et al., 2019), PEARL (Rakelly et al., 2019), VariBAD (Zintgraf et al., 2019), and Meta-DT (Wang et al., 2024). ANIL (Raghu et al., 2019) is implemented by modifying our MAML code to freeze the feature backbone during adaptation (inner loop), while keeping the head trainable; we otherwise reuse the same meta-training and adaptation hyperparameters as in MAML. For a fair comparison, we keep the policy network size (hidden depth and units per layer) identical across all methods.